

## ON LASER RADAR CROSS SECTION OF TARGETS WITH LARGE SIZES FOR E-POLARIZATION

H. El-Ocla

Department of Computer Science  
Lakehead University  
955 Oliver Road, Thunder Bay, Ontario P7B 5E1, Canada

**Abstract**—In this paper a study is presented to handle the behavior of radar cross section (RCS) of partially convex targets of large sizes up to five wavelengths in free space. The nature of incident wave is an important factor in the remote sensing and radar detection applications. To investigate the effects of incident wave nature on the RCS, scattering problems of plane and beam wave incidences are considered. Targets are taking large sizes to be bigger enough than the beam width with putting into consideration a horizontal incident wave polarization (E-wave incidence). The effects of the target configuration together with the beam width on the laser RCS compared to the case with the plane wave incidence are numerically analyzed. Therefore, we will be able to have some sort of control on radar detection using beam wave incidence.

### 1. INTRODUCTION

The radar scattering from electrically real targets of finite sizes remains a very challenging problem in computational electromagnetics. Some methods proposed to formulate the scattering wave were presented: examples are in [1–3]. In this regard, some years ago, a method has been presented for solving the scattering problem as a boundary value problem [4–8]. This method is characterized by the estimation of the current on the whole surface and not only on the illumination region as in the physical optics method. Therefore this method gives a precious calculation of the wave intensity.

Numerical results have been shown for RCS of conducting convex bodies such as circular and elliptic cylinders [4]. Later as the more practical models, the effects of target configuration and polarization on the radar cross section (RCS) were analyzed in many of my publications

(e.g., [5–8], where other references are available). It was found that the target configuration together with incident wave polarization obviously affect the RCS.

It should be noted that for generating waves of infinitely large plane wave fronts, an infinitely large source should be used. This can not be available easily especially for plane waves wide sufficiently at the fronts of large size targets in the far field. In an attempt to generate plane wave, an expansion of plane wave into Gaussian beam waves was derived [9]. Gaussian beams play a key role in different fields of physics; let us mention applications in lasers, electromagnetic waves, etc. Many problems of propagation and scattering of Gaussian beams have been solved (see [6, 10, 11], where other references can be found). On the other hand, the research on laser radar [12] for target ranging, detection, and recognition [13] has become the one key technology to evaluate and model the characteristics of scattering from a complex target in the military and civil applications.

In this regard, the scattering characteristics are analyzed through studying the behavior of laser RCS (LRCS) of the target. In doing that, one can calculate the LRCS by assuming a beam wave incident on a nonconvex target in free space. In fact, we can consider the beam wave as a plane wave when the mean size of the target becomes smaller than the beam width, however, this is not usually the general case practically. To detect targets of larger sizes, we should, therefore, handle the case where the beam width is smaller than the target size.

Here, we evaluate the effects of the target configuration including size and curvature on the RCS of target for the two cases of plane and beam wave incidences. To achieve this aim, we draw on our method described earlier to conduct numerical results for the RCS of concave-convex targets of large sizes up to about five wavelengths to be bigger enough than the beam width. Next, we estimate the normalized RCS (NRCS), defined as the ratio of LRCS  $\sigma_b$  to RCS for plane wave incidence  $\sigma_0$ . Therefore, we will be able to analyze the difference in the behavior between RCS and LRCS. I consider the case where a directly incident wave is produced by a line source distributed uniformly along the axis parallel to the conducting cylinder (target) axis. Then we can deal with this scattering problem two-dimensionally with assuming horizontal polarization (E-wave incidence). In the previous work [5, 7], it has been clarified that the RCS changes obviously with the illumination region curvature. In this study, it is concentrated on the wave backscattering from convex illumination portion only. The time factor  $\exp(-i\omega t)$  is assumed and suppressed in the following section.

## 2. FORMULATION

Let us consider scattering waves from targets with assuming two cases: (1) plane wave incidence, (2) beam waves incidence, in free space. For both scattering problems, geometry of the problem is shown in Figure 1. Here,  $k = \omega\sqrt{\varepsilon_0\mu_0}$  is the wavenumber in free space where  $\varepsilon_0$  and  $\mu_0$  are the free space permittivity and magnetic permeability, respectively, and  $W$  is the beam width.

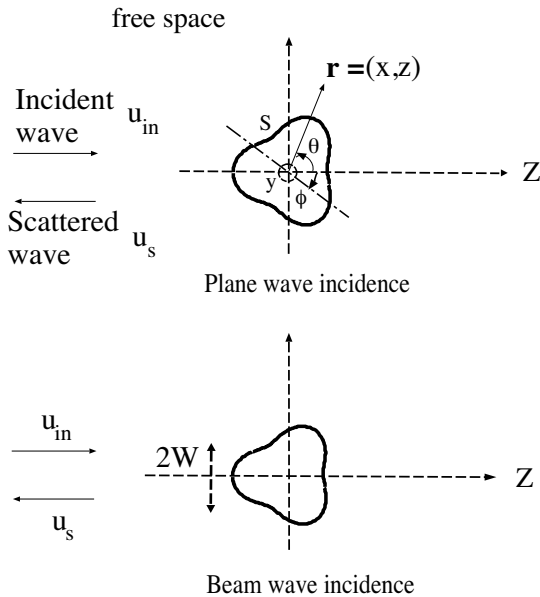


**Figure 1.** Geometry of the problem of wave scattering from a conducting cylinder.

Consider the case where a directly incident wave is produced by a line source  $f(\mathbf{r}')$  distributed uniformly along the  $y$  axis. Then, the incident wave is cylindrical and becomes plane approximately around the target because the line source is very far from the target. Here, let us designate the incident wave by  $u_{in}(\mathbf{r})$ , the scattered wave by  $u_s(\mathbf{r})$ , and the total wave by  $u(\mathbf{r}) = u_{in}(\mathbf{r}) + u_s(\mathbf{r})$ . An electromagnetic wave radiated from the line source located at  $\mathbf{r}_t$  propagates in free space, illuminates the target and induces a surface current on the target. A scattered wave from the target is produced by the surface current and propagates back to the observation point that coincides with the source point.

The target is assumed as a conducting cylinder. The cross-section

of the cylinder is expressed by

$$r = a[1 - \delta \cos 3(\theta - \phi)] \quad (1)$$

where  $a$  is the mean size of the target in which  $a \ll \mathbf{r}_t$ ,  $\delta$  is the concavity index, and  $\phi$  is the rotation index which represents the incident angle.

Using the current generators  $Y_E$  and Green's function in free space  $G_0(\mathbf{r} | \mathbf{r}')$ , we can express the scattered wave as

$$u_s(\mathbf{r}) = \int_S d\mathbf{r}_1 \int_S d\mathbf{r}_2 [G_0(\mathbf{r} | \mathbf{r}_2) Y_E(\mathbf{r}_2 | \mathbf{r}_1) u_{in}(\mathbf{r}_1 | \mathbf{r}_t)] \quad (2)$$

For the scattering problem with plane wave incidence,  $u_{in}(\mathbf{r}_1 | \mathbf{r}_t)$  is expressed as

$$u_{in}(\mathbf{r}_1 | \mathbf{r}_t) = G_0(\mathbf{r}_1 | \mathbf{r}_t) \quad (3)$$

whose dimension coefficient is understood. Here  $Y_E$  is the operator that transforms incident waves into surface currents on  $S$  and depends only on the scattering body [4–8]. The current generator can be expressed in terms of wavefunctions, which satisfy Helmholtz equation and the radiation condition. That is, for E-wave incidence, the current generator is obtained as

$$Y_E(\mathbf{r} | \mathbf{r}') \simeq \Phi_M^*(\mathbf{r}) A_E^{-1} \ll \Phi_M^T(\mathbf{r}') \quad (4)$$

where  $\Phi_M = [\phi_{-N}, \phi_{-N+1}, \dots, \phi_N]$ ,  $M = 2N + 1$  is the total mode number,  $\phi_m(\mathbf{r}) = H_m^{(1)}(k\rho) \exp(im\theta)$ , and  $A_E$  is a positive definite Hermitian matrix given by

$$A_E = \begin{pmatrix} (\phi_1, \phi_1) & \dots & (\phi_1, \phi_M) \\ \vdots & \ddots & \vdots \\ (\phi_M, \phi_1) & \dots & (\phi_M, \phi_M) \end{pmatrix} \quad (5)$$

in which its  $m, n$  element is the inner product of  $\phi_m$  and  $\phi_n$ :

$$(\phi_m, \phi_n) \equiv \int_S \phi_m(\mathbf{r}) \phi_n^*(\mathbf{r}) d\mathbf{r} \quad (6)$$

where  $\ll \Phi_M^T$ , denotes the operation (7) of each element of  $\Phi_M^T$  and the function  $u_{in}$  to the right of  $\Phi_M^T$

$$\ll \phi_m(\mathbf{r}), u_{in}(\mathbf{r}) \gg \equiv \phi_m(\mathbf{r}) \frac{\partial u_{in}(\mathbf{r})}{\partial n} - \frac{\partial \phi_m(\mathbf{r})}{\partial n} u_{in}(\mathbf{r}). \quad (7)$$

The  $Y_E$  is proved to converge in the sense of mean on true operators when  $M \rightarrow \infty$ .

For the scattering problem with Gaussian beam wave incidence, let us consider  $u_{in}(\mathbf{r}_1 | \mathbf{r}_t)$  to be represented by

$$u_{in}(\mathbf{r}_1 | \mathbf{r}_t) = G_0(\mathbf{r}_1 | \mathbf{r}_t) \exp \left[ - \left( \frac{kx_1}{kW} \right)^2 \right] \quad (8)$$

The beam expression is approximately useful only around the cylinder.

The plane wave can be considered as a beam wave with infinite beam width, that is:

$$W = \infty \quad \text{for plane wave incidence} \quad (9)$$

We can obtain the RCS  $\sigma_0$  for plane wave incidence using equations (2) and (3), and obtain LRCS  $\sigma_b$  using equations (2) and (8). We use  $\sigma$  as a general symbol that indicates both  $\sigma_0$  and  $\sigma_b$  and can be calculated as

$$\sigma = |u_s(\mathbf{r})|^2 k(4\pi z)^2. \quad (10)$$

### 3. NUMERICAL RESULTS

Here, we point out that  $N$ , in the formulation, depends on the target parameters. For example, we choose  $N = 24$  at  $\delta = 0.1$  in the range of  $0.1 < ka < 5$ ; at  $ka = 20$ , we choose  $N = 40$  at  $\delta = 0.1$ . As a result, our numerical results are accurate because these values of  $N$  lead to convergent RCS. In the numerical results, it is assumed that  $\phi = \pi$ .

Let us define the effective illumination region (EIR<sub>p</sub>) as that surface that is illuminated by the plane wave incidence as shown in Figure 2-a. On the other hand, we define the effective illumination region (EIR<sub>b</sub>) as that surface that is illuminated by the beam wave incidence and restricted by the  $2kW$  as shown in Figure 2-b. According to (9) and as shown in Figure 2, EIR<sub>p</sub> > EIR<sub>b</sub>, which results in increase in the surface current generated and that leads to the relation:  $\sigma_0 > \sigma_b$ , as we are going to see in the numerical results. Also, from Figure 2, we expect that the target configuration including  $\delta$  and  $ka$  together with  $kW$  are going to affect the EIR generally. Accordingly, the RCS, LRCS, and the enhancement factor of NRCS will be influenced by a way that will be clarified in the numerical results.

We define DRCS as the difference in the behavior of RCS  $\sigma$  with  $ka$  between plane and beam wave incidences, i.e., between  $\sigma_0$  and  $\sigma_b$ . To detect the target through calculating its RCS, the target should be surrounded by the incident wave. This condition is realized with the plane wave but not with the beam wave since the later illuminates only a portion of the target. Therefore the beam wave does not cause

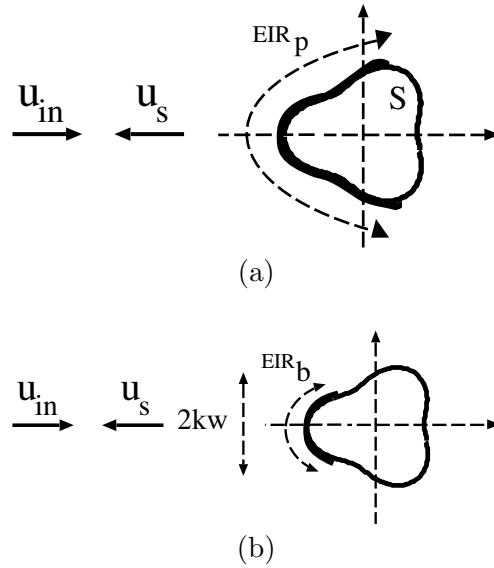


**Figure 2.** Geometry shows the effective illumination region where (a) plane wave incidence, (b) beam wave incidence.

generating enough surface current needed for correct RCS calculation. Accordingly, as the DRCS decreases, as the estimated RCS becomes more accurate. In the following sections, a numerical analysis for the parameters that affect the DRCS is going to be presented.

### 3.1. Radar Cross-section RCS

Here, I discuss the numerical results for  $\sigma_0$  and  $\sigma_b$  shown in Figures 3 and 4. We notice from these figures that there are two effects on both  $\sigma_0$  and  $\sigma_b$ . The first is the effect of target configuration and can be seen clearly with changing  $\delta$  and  $ka$  as shown in Figure 3. For small  $ka$  and/or large  $\delta$ , DRCS becomes small. As  $ka$  increases and/or  $\delta$  decreases, as the DRCS increases due to the lack in EIR<sub>b</sub>, and vice versa. To understand such behavior, we have to turn the attention to that in case of beam wave incidence, the surface current outside EIR<sub>b</sub> is relatively small compared to that at the beam spot that is inside the EIR<sub>b</sub>. Therefore in accordance to (2), as EIR<sub>b</sub> shrinks, as the contribution to the scattered waves decreases effectively.

The second is the effect of the beam width size  $kW$  shown in Figure 4. Note that there is a direct relationship between  $\sigma_b$  and  $kW$ . In other words, when  $kW$  increases, the results of  $\sigma_b$  become closer to

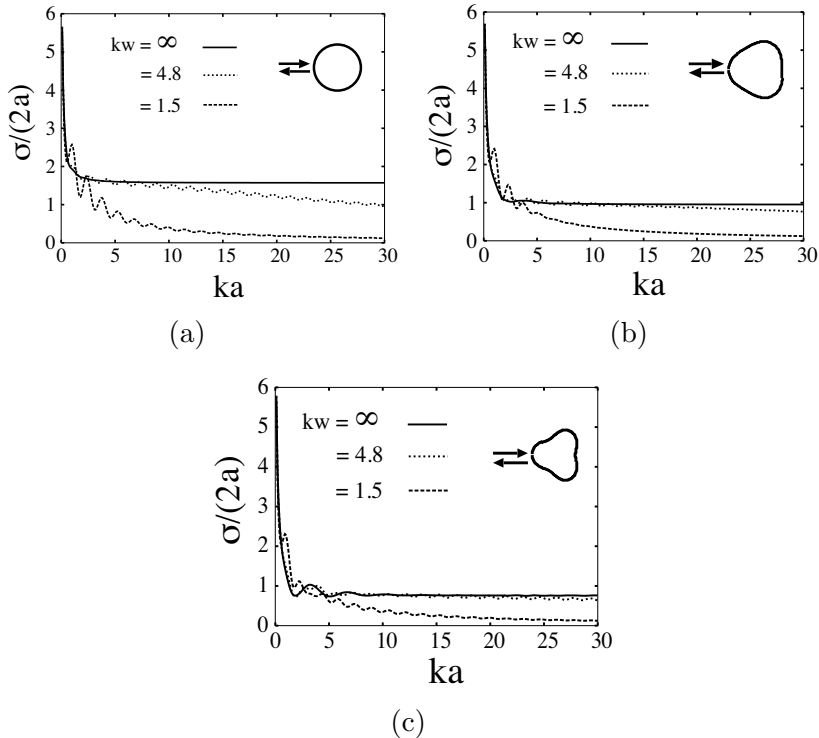


**Figure 3.** RCS vs. target size for E-wave incidence in free space where (a)  $\delta = 0$ , (b)  $\delta = 0.1$ , and (c)  $\delta = 0.2$ .

$\sigma_0$  and that agrees with the conclusion published in [14].

In Figure 4-a,  $\sigma_0$  is invariant with  $ka$  because the generated surface current does not change since the illumination region is always covered by the plane wave incidence. In contrast, with increasing  $ka$  in Figures 4-b,c,  $\sigma_b$  decreases as a result of the shortage in the surface current and that leads to the gradual decrease in the scattered wave contribution with  $ka$  as explained above. Also, it is observed that  $\sigma_b$  differs with  $\delta$  for small  $ka$  and absolutely coincides with larger  $ka$ . The coincidence of  $\sigma_b$  becomes more obvious and earlier with  $ka$  for smaller  $kw$ . This occurs when  $ka \gg kW$  in which the surface current outside  $EIR_b$  has a slight contribution to the scattered waves with different  $\delta$ . At certain limit,  $\sigma_b$  will diminish with large enough target and the beam wave becomes incapable of target detection.

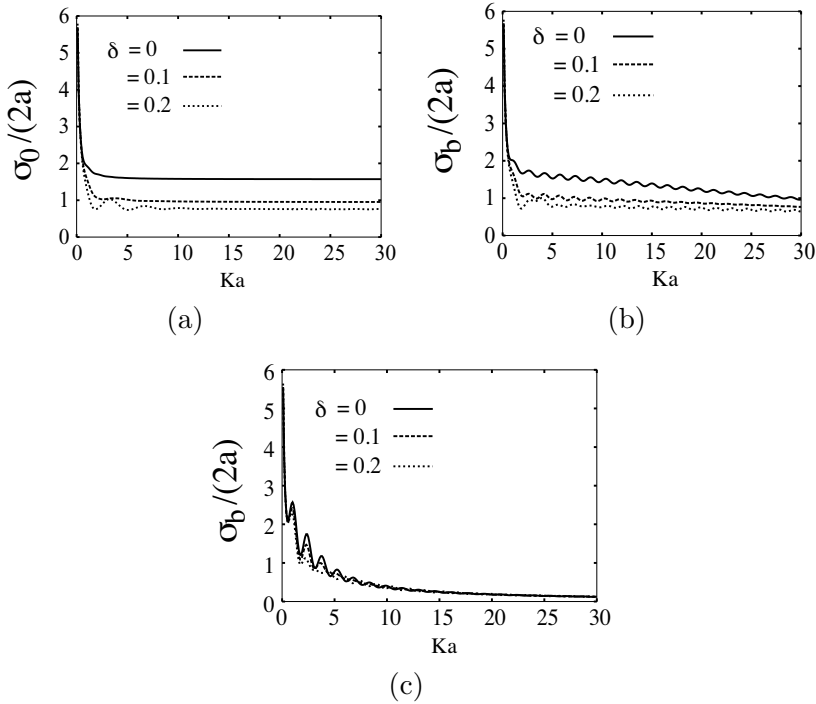


**Figure 4.** RCS vs. target size for different  $\delta$  where (a) plane wave incidence ( $kW = \infty$ ), (b) beam wave incidence with  $kW = 4.8$ , and (c) beam wave incidence with  $kW = 1.5$ .

### 3.2. Normalized Radar Cross-section

Here NRCS, defined as the ratio of LRCS  $\sigma_b$  to RCS for plane wave incidence  $\sigma_0$ , is considered to manifest the DRCS and hence numerical results for NRCS are presented in Figure 5.

NRCS is analyzed in three regions of  $ka$  compared to  $kW$ .

For  $ka \ll kW$ , the NRCS equals one and this value of NRCS is realized, independent of illumination portion curvature, i.e., independent of the concavity index  $\delta$ . In this range, beam wave seems as if it is a plane wave for the small  $ka$  and therefore DRCS equals zero.

For  $ka \simeq kW$ , the NRCS oscillates remarkably and irregularly far from one. In fact, this irregular oscillation, that decreases with  $\delta$ , is due to the DRCS. However, the strength of this oscillation, i.e. enhancement factor, in NRCS decreases with increasing  $kW$  which in turn reduces DRCS.



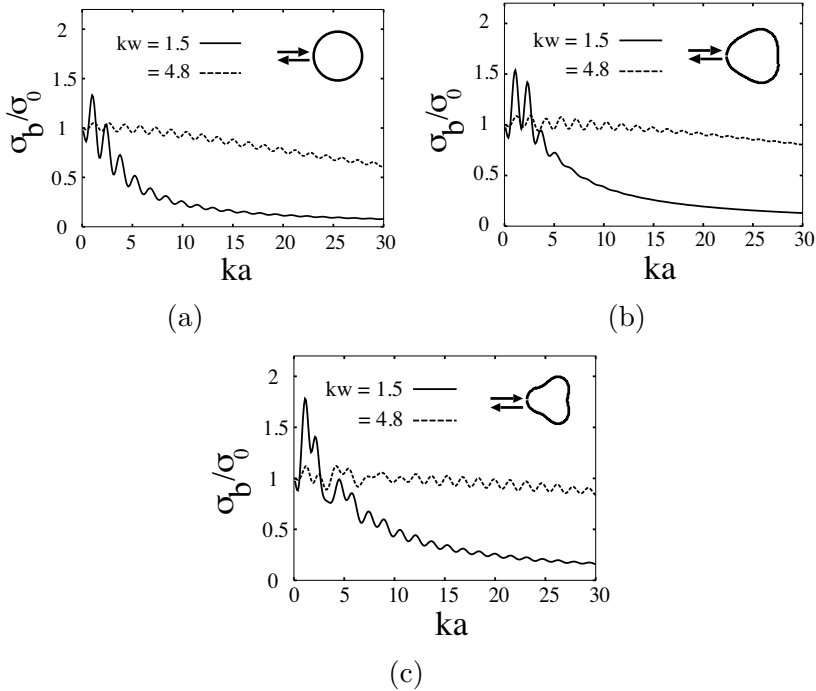


**Figure 5.** Normalized RCS vs. target size for E-wave incidence in free space where (a)  $\delta = 0$ , (b)  $\delta = 0.1$ , (c)  $\delta = 0.2$ .

For  $ka > kw$ , NRCS decreases gradually with  $ka$ ; this decrease is faster with smaller  $kw$ , this behavior is due to the DRCS as illustrated earlier. In the region  $ka \gg kw$ , the impact of  $\delta$  becomes fairly limited on the EIR, as has been explained previously, and therefore the amount of scattered waves changes slightly. Accordingly, the decrease behavior of RCS becomes quite similar with different  $\delta$  for large  $ka$ .

#### 4. CONCLUSION

The behavior of RCS of partially convex targets taking large sizes up to five wavelengths in free space was evaluated. The scattering problems of plane and beam wave incidences were considered. In this study, we clarified the effects of the target configuration together with beam width on the laser RCS (LRCS) compared to the case with plane wave incidence. When target size becomes larger enough than the beam width, it was found that target curvature has a slight effect on the LRCS behavior. On the other hand of the later case, the LRCS

was proved to differ obviously from RCS for plane wave incidence and that difference increases with target size. At certain limit, LRCS will diminish with large enough target and the beam wave incidence becomes incapable of target detection. For larger beam width, LRCS becomes closer to RCS for plane wave incidence, however, it changes obviously with target curvature.

## ACKNOWLEDGMENT

This work was supported in part by National Science and Engineering Research Council of Canada (NSERC) under Grant 250299-02.

## REFERENCES

1. Keller, J. B. and W. Streifer, "Complex rays with an application to Gaussian beams," *J. Opt. Soc. Am.*, Vol. 61, No. 1, 40–43, 1971.
2. Ikuno, H., "Calculation of far-scattered fields by the method of stationary phase," *IEEE Transactions on Antennas and Propagation*, Vol. AP-27, No. 2, 199–202, 1979.
3. Mieras, B. C. L., "Time domain scattering from open thin conducting surfaces," *Radio Science*, Vol. 16, No. 6, 1231–1239, 1981.
4. Meng, Z. Q. and M. Tateiba, "Radar cross sections of conducting elliptic cylinders embedded in strong continuous random media," *Waves in Random Media*, Vol. 6, 335–345, 1996.
5. El-Ocla, H. and M. Tateiba, "Strong backscattering enhancement for partially convex targets in random media," *Waves in Random Media*, Vol. 11, No. 1, 21–32, 2001.
6. El-Ocla, H. and M. Tateiba, "An indirect estimate of RCS of conducting cylinder in random medium," *IEEE Antennas and Wireless Propagation Letters*, Vol. 2, 173–176, 2003.
7. El-Ocla, H. and M. Tateiba, "Numerical analysis of some scattering problems in continuous random medium," *Progress in Electromagnetics Research*, PIER 42, 107–130, (Abstract in *Journal of Electromagnetic Waves and Applications*, Vol. 17, No. 10, 1421–1422), EMW, Cambridge, MA, 2003.
8. El-Ocla, H., "Backscattering from conducting targets in continuous random media for circular polarization," *Waves in Random Media*, Vol. 15, 2005.
9. Cerveny, V., "Expansion of a plane wave into Gaussian beams," *Studia Geophysica et Geodaetica*, Vol. 46, Suppl. Special Issue, 43–54, 2002.

10. Gardner, J. S. and R. E. Collin, "Scattering of a Gaussian laser beam by a large perfectly conducting cylinder: physical optics and exact solutions," *IEEE Transactions on Antennas and Propagation*, Vol. 52, No. 3, 642–652, 2004.
11. Sakurai, H., M. Ohki, K. Motojima, and S. Kozaki, "Scattering of Gaussian beam from a hemispherical boss on a conducting plane," *IEEE Transactions on Antennas and Propagation*, Vol. 52, No. 3, 892–894, 2004.
12. Jelalian, A. V., *Laser Radar Systems*, Artech House, Boston, Mass., 1992.
13. Steinvall, O., H. Olsson, G. Bolander, C. Carlsson, and D. Letalick, "Gated viewing for target detection and recognition," *Laser Radar Technology and Applications IV*, G. W. Kamerman and C. Werner (eds.), *Proc. SPIE 3707*, 432–448, 1999.
14. Peng, M. Y. and W. B. Dou, "Diffraction of Gaussian beam by a periodic screen," *International Journal of Infrared and Millimeter Waves*, Vol. 22, No. 8, 1277–1286, 2001.